A Membrane-Mimetic Barrier for Cell Encapsulation

Hongbo Liu,[†] Keith M. Faucher,[†] Xue-Long Sun,[†] June Feng,[†] Tiffany L. Johnson,[†] Janine M. Orban,[†] Robert P. Apkarian,[‡] Richard A. Dluhy,[§] and Elliot L. Chaikof*[,†,⊥]

Departments of Bioengineering, Surgery, and Chemistry, Emory University School of Medicine, Atlanta, Georgia 30322, School of Chemical Engineering, Georgia Institute of Technology, Atlanta, Georgia 30320, and Department of Chemistry, University of Georgia−Athens, Athens, Georgia 30602

Received August 7, 2001. In Final Form: November 7, 2001

A stabilized, membrane-mimetic film was produced on a polyelectrolyte multiplayer (PEM) by in-situ photopolymerization of an acrylate functonalized phospholipid assembly at a solid−liquid interface. The phospholipid monomer was synthesized, prepared as unilamellar vesicles, and fused onto close-packed octadecyl chains as part of an amphiphilic terpolymer anchored onto the PEM by electrostatic interactions. The lipid film displayed an advancing contact angle of ∼ 60°, elemental composition, as determined by X-ray photoelectron spectroscopy, was in agreement with that anticipated for a lipid membrane. Data obtained from both high-resolution scanning electron microscopy and ellipsometry were consistent with the formation of a supported lipid monolayer. In addition, polarized external reflection infrared spectroscopy revealed significant acyl chain ordering induced on lipid fusion and polymerization. Doping the lipid assembly with a fluorescein terminated polymerizable lipid provided visible confirmation of film formation and its stability under a variety of conditions, including shear rates of 2000 sec^{-1}. Transport studies demonstrated that the addition of a lipid film significantly reduced barrier permeability for compounds in excess of 70 kD. The ability to coat microbeads ($d \sim 300\ \mu m$) with a robust membrane-mimetic film, while preserving encapsulated cell viability is illustrated, thereby establishing a new strategy for modulating the physiochemical and biological properties of immunoisolation barriers for cell transplantation.

Supported lipid membranes can be produced by assembling a layer of closely packed hydrocarbon chains onto an underlying substrate followed either by controlled dipping through an organic amphiphilic monolayer at an air−water interface or by exposure to a dilute solution of emulsified lipids or unilamellar lipid vesicles[1]. In the process of membrane formation, the functional reconstitution of integral or membrane-anchored proteins can be readily achieved. As a consequence, supported lipid membranes have proven to be useful tools for characterizing both protein function and cell−cell interactions. Moreover, interest has been generated in the potential application of supported membranes as sensors or biofunctional coatings for artificial organs and other implanted medical devices.[1,2]

A significant limitation in the widespread use of supported biomembranes, however, remains their limited stability for most applications outside of a laboratory environment. To generate more robust systems, strategies have been developed to tether membranes to an underlying substrate, such as gold or glass with or without an intervening flexible spacer or polymer cushion.[3−8] While membrane fluidity is critical for many of the functional responses of biological membranes, certain applications lend themselves to compromise, in which a substantial increase in membrane stability may be achieved by in-situ polymerization of the planar lipid assembly, admittedly at the expense of reducing lateral mobility. While not necessarily an ideal solution, the capacity to design surfaces with a high degree of molecular control over the *assembly* of diverse lipid and other membrane-associated constituents is retained. In this regard, we have previously reported the in-situ polymerization of phospholipids on self-assembled monolayers of octadecyl mercaptan bound to gold,[9] octadecyl trichlorosilane on glass,[10,11] and on an amphiphilic polymer cushion.[12]

Recently, polyelectrolyte multilayers have been studied as bioinert films to reduce cell and protein adhesion[13] and as coatings to modulate interfacial molecular transport in drug delivery and immunoisolation systems.[14,15] Other potential applications for these materials include their

* To whom correspondence should be addressed: 1639 Pierce Drive, Room 5105, Emory University, Atlanta, GA 30322. Phone (404) 727-8413. Fax: (404) 727−3660. E-mail: echaiko@emory.edu.

[†] Department of Bioengineering, Emory University School of Medicine.

[‡] Department of Chemistry, Emory University School of Medicine.

[§] Department of Chemistry, University of Georgia-Athens.

[⊥] School of Chemical Engineering, Georgia Institute of Technology.

(1) Sackmann, E. *Science* **1996**, *271*, 43−48.
(2) Marra, K. C.; Winger, T. M.; Hanson, S. R.; Chaikof, E. L. *Macromolecules* **1997**, *30*, 6483−6487.
(3) Spinke, J. Y.; Wolf, H.; Liley, M.; Ringsdorf, H.; Knoll, W. *Biophys. J.* **1992**, *63*, 1667−1671.
(4) Florin, E.-L.; Gaub, H. E. *Biophys. J.* **1993**, *64*, 375−383.
(5) Meuse, C. W.; Krueger, S.; Majkrzak, C. F.; Dura, J. A.; Fu, J.; Connor, J. T.; Plant, A. L. *Biophys. J.* **1998**, *74*, 1388−1398.
(6) Seitz, M,; Wong, J. Y.; Park, C. K.; Alcantar, N. A.; Israelachvili, J. *Thin Solid Films* **1998**, *329*, 767−771.
(7) Beyer, D.; Knoll, W.; Ringsdorf, H.; Elender, G.; Sackmann E. *Thin Solid Films* **1996**, *285*, 825−828.
(8) Shen, W. W.; Boxer, S. G.; Knoll, W.; Frank, C. W. *Biomacromolecules* **2001**, *2*, 70−79.
(9) Marra, K. G.; Kidani, D. D. A.; Chaikof, E. L. *Langmuir* **1997**, *13*, 5697−5701.
(10) Marra, K. G.; Winger, T. M.; Hanson, S. R.; Chaikof, E. L. *Macromolecules* **1997,** *30*, 6483−6488.
(11) Orban J. M.; Faucher, K. M.; Dluhy, R. A.; Chaikof, E. L. *Macromolecules* **2000**, *33*, 4205−4212.
(12) Chon, J. H.; Marra, K. G.; Chaikof, E. L. *J. Biomat. Sci. Polymer. Ed.* **1999**, *10*, 95−108.
(13) Elbert, D. L.; Herbert, C. B.; Hubbell, J. A. *Langmuir* **1999,** 15, 5355−5362.
(14) Moya, S.; Donath, E.; Sukhorukov, G. B.; Auch, M.; Baumler, H.; Lichtenfeld, H.; Mohwald, H. *Macromolecules* **2000**, *33*, 4538−4544
(15) Shi, X.; Caruso, F. *Langmuir* **2001**, *17*, 2036−2042.

10.1021/la011254g CCC: $22.00
Published on Web 01/26/2002

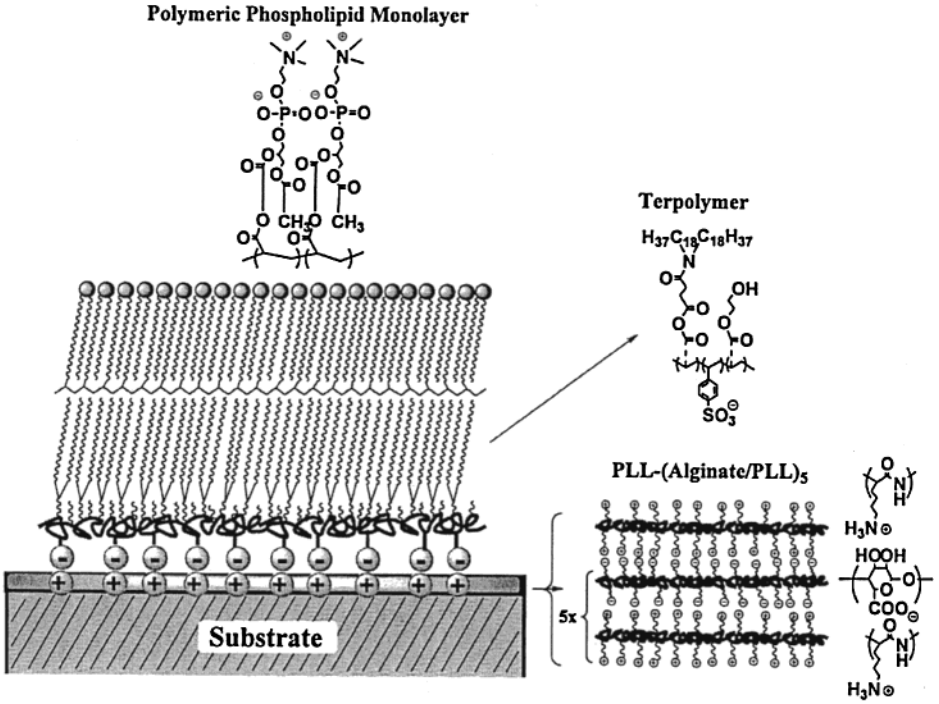

Figure 1. Schematic representation of polymeric phospholipid monolayer supported on a polyelectrolytes multilayer.

use as ultrafiltration membranes[16] and in the assembly of optoelectronic devices.[17] We believe that the formation of a *stabilized* lipid membrane on a polyelectrolyte multilayer will significantly enhance the versatility of these systems by offering an additional mechanism for modulating both the surface physiochemical properties and biological activity of the film. Indeed, Kiser et al.[18] and Moya et al.[14] have noted that lipid assemblies adsorbed onto the surface of a polyelectrolyte can reduce the release of doxorubicin and 6-carboxyfluorescein, respectively. In this report, we describe a new approach for generating a robust, membrane-mimetic coating on a polyelectrolyte multilayer (Figure 1). Briefly, we designed an amphiphilic polymer with anionic anchoring groups that provided a convenient means for surface alkylation with an intervening polymer cushion. Following the formation of a surface supported assembly of mono-acrylated lipids, photoinitiated polymerization was performed to stabilize the membrane. The molecular characteristics of this system were characterized, its inherent stability in a high shear rate environment confirmed, and its capacity to modulate interfacial molecular transport demonstrated. In addition, the ability to use this system as a cell encapsulation barrier is illustrated.

Materials and Methods

Reagents. All starting materials and synthetic reagents were purchased from commercial suppliers unless otherwise noted. Poly-L-lysine (PLL; 21−479 kD) was purchased from Sigma. Alginate (ca. 41% guluronic acid) was obtained from ISP alginate (San Diego, CA) and used as received. *N*,*N*-dioctadecylcarbamoyl propionic acid (DOD), poly(HEA-DOD)$_{6:3}$, 1-palmitoyl-2-(12-(acryloyloxy)dodecanoyl)-*sn*-glycero-3-phosphorylcholine (mono-AcrylPC), and 1-palmitoyl-2-(12-(acryloyloxy)-dodecanoyl)-sn-glycero-3-phosphorylethanolamin e-fluorescein isothiocyanate were synthesized as previously described.[10,12,19,20]

Instrumentation. *Ellipsometry* data was obtained using a PlasMos ellipsometer, Model SD2300 equipped with a HeNe laser as a light source. The light was incident at an angle of 70° to the surface normal. The organic layer was assumed to have a refractive index *n* of 1.45.

High-Resolution Scanning Electon Micrographs (HR−SEM) were obtained using an in-lens field emission scanning electron microscope (ISI DS-130F Schottky Field Emission SEM) that was operated at 5 kV. Sample-containing silicon chips were mounted onto aluminum specimen stubs with silver paste, degassed for 30 min, and coated with a 1 nm chromium (Cr) film.

^1H and ^{13}C NMR Spectra were recorded at room temperature with a Varian INOVA 400 spectrometer (magnetic field strengths of 400 and 100 MHz for ^{1}H and ^{13}C NMR analyses, respectively). *Mass spectra* (MS/FAB) were obtained at an ionizing voltage of 70 eV.

The Size-Exclusion Chromatography (SEC) equipment consisted of a Waters model 510 HPLC pump, Waters Ultrahydrogel 250 and 2000 columns, and a Wyatt Technology Optilab 903 refractometer. The actual molar masses of the polymer samples were determined from the response of the DAWN F multiangle laser light-scattering (LLS) detector (Wyatt Technology) that was connected to the outlet of the SEC apparatus.

Contact Angles were obtained using a Rame-Hart goniometer, Model 100-00. Measurements are reported as average value of advancing or receding contact angles of at least 15 data points (5 measurements each per three samples).

Angle-Dependent ESCA was performed using a Physical Electronics (PHI) model 5100 spectrometer equipped with a Mg−Ti dual-anode source and an Al−Be window. The system uses a hemispherical analyzer with a single-channel detector. Spectra were obtained at the following takeoff angles: 15°, 45°, and 90°.

(16) van Ackern, F.; Krasemann, L.; Tieke, B. *Thin Solid Films* **1998**, *329*, 762−766.
(17) Cheung, J. H.; Fou, A. F.; Rubner, M. F. *Thin Solid Films* **1994**, *244*, 985.
(18) Kiser, P. F.; Wilson, G.; Needham, D. *Nature* **1998**, *394*, 459−62.
(19) Sells, T. D.; O'Brien, D. F. *Macromolecules* **1994,** *27*, 226−233.
(20) Sun, X.-L.; Liu, H.; Orban, J. M.; Sun, L.; Chaikof, E. L. *Bioconjugate Chemistry* **2001**, *12*, 673−677.

Infrared Spectroscopy. Spectra were acquired using a BioRad FTS-60 Fourier Transform Infrared (FT-IR) spectrometer equipped with a wide band MCT detector, collected with 1024 scans, triangular apodization, and 4 cm^{-1} resolution. Polarized infrared external reflection spectra were obtained using a Harrick external reflection accessory (60° angle of incidence; Ossining, NY) with infrared radiation polarized perpendicular or parallel to the surface normal using a Molectron ZnSe wire grid polarizer (Portland, OR). The spectrum of a clean silicon wafer was used to determine the background.

Fluorescence Microscopy. Fluorescence images were acquired using a Zeiss epifluorescence microscope under 50X magnification, illuminated with a xenon−mercury arc lamp, and a low light level Hamamatsu SIT camera detector. Images were acquired for films deposited on Si substrates.

Preparation of Glass Substrates. Glass slides were purchased from Fisher as 18 mm circular disks with a nominal thickness of 0.17−0.23 mm. Slides were cleaned prior to use by sonication in a 1:8 mixture of Multi-Terge detergent (EM Diagnostic Systems, Gibbstown, NJ) and deioinized water for 20 min, followed by additional rinsing with water and a second 20 min period of sonication in water.

Statistical Copolymerization of 2-Hydroxyethyl Acrylate (HEA) and Styrene Sulfonate (SSS). HEA (1.15 mL; 10 mmol) and SSS (0.206 g; 1.0 mmol) were dissolved into 20 mL dimethyl sulfoxide. 2,2′-Azobisisobutyronitrile (AIBN; 18 mg; 0.11 mmol) was added, the solution purged with N_2 for 30 min, and the reaction mixture placed in a 70 °C oil bath for 20 h. The reaction mixture was slowly added to 400 mL of cold CH_2Cl_2 with vigorous stirring. A colorless glue-like precipitate formed and the solid rinsed twice with CH_2Cl_2 prior to overnight drying under vacuum. The final product was a white solid that was highly hygroscopic and was referred to as poly-(HEA-SSS)$_{10:1}$. Yield: (1.16 g, 85%). ^{1}H NMR (CD_3OD), δ: 3.99 (2H, CH_2 of HEA), 7.50 and 7.04 (4 H, Ar−H of SSS). ^{1}H NMR (DMSO-*d*6), δ: 7.50 (br, Ar−H); 7.04 (br, Ar−H); 3.99 (br, CH2−O−C═O); 3.54 (br, CH2−OH); 2.54 (br., CH); 2.25 (br, CH2). GPC (LLS): Mn = 25,300, PDI = 1.75.

Synthesis of an HEA-SSS-DOD Terpolymer. Poly-(HEA-*co*-SSS) $_{10:1}$ (0.410 g; 3.0 mmol of HEA mer-unit) was dissolved in 15 mL dimethylformamide (DMF) and later diluted with 10 mL of CH_2Cl_2. *N*,*N*-dioctadecylcarbamoyl-propionic acid (DOD; 0.652 g; 1.05 mmol) in 10 mL of CH_2Cl_2 was slowly added to the above solution followed by the addition of *p*-dimethyl aminopyridine (12.8 mg; 0.11 mmol). A small volume of DMF (ca. 0.5 mL) was added to maintain clarity of the solution, the reaction mixture placed in an ice−water bath, and dicyclohexylcarbodiimide (0.284 g, 1.38 mmol) in 3 mL of CH_2Cl_2 was added dropwise. The reaction proceeded overnight under N_2. The reaction mixture was then evaporated to dryness and mixed with 20 mL of diethyl ether. The mixture was filtered, the filtrate evaporated to dryness, dissolved in 5 mL of CH_2Cl_2, and the polymer precipitated in 100 mL of acetonitrile. The product was a white powder and ^{1}H NMR and elemental analysis confirmed a monomer ratio in the terpolymer of HEA:DOD:SSS of 6:3:1. This compound was referred to as poly(HEA_6:DOD_3:SSS_1). Yield: 0.770 g, 73%. ^{1}H NMR ($CDCl_3$), δ: 4.27 (br., CH_2–O−C═O); 3.76 (br. CH_2–OH); 3.22 (br. CH_2–N−C═O); 2.62 (br., CH_2–C═O, CH−Ar); 2.39 (br., CH_2, CH); 1.56 (br., CH_2); 1.47 (br., CH_2); 1.25 (br., CH_2); 0.87 (br., CH_3). IR (KBr pellet): 1732 cm^{-1} (O═C−O-), 1649 cm^{-1} (O═C−N). GPC (LLS): Mn = 49,800, PDI = 1.80. Elemental analysis: Calculated: 67.83% C, 10.20% H, 18.80% O, 1.37% N; 1.04% S; Observed: 67.54% C, 10.28% H, 18.77% O, 1.80% N, 0.96% S.

Preparation of (PLL-alginate)$_5$-PLL-Polymer Films on Glass. PLL and alginate were prepared at concentrations of 0.10 w/v % and 0.15 w/v % in phosphate buffered saline (PBS), respectively. In the generation of a polyelectrolyte multilayer, contact times were approximately 30 s for each solution and surfaces were rinsed three times ($\sim$ 10 s/rinse) with water between each coating solution. (PLL-alg)$_5$–PLL coated glass slides were exposed to solutions of either poly(HEA-DOD)$_{6:3}$ or poly(HEA-DOD-SSS)$_{6:3:1}$ in triethylene glycol (TEG) at concentrations of 3 mmol of DOD or 1 mmol SSS, respectively. Poly(HEA-DOD)$_{6:3}$ was used to determine whether the styrene sulfonate groups were the primary determinants of poly-(HEA-DOD-SSS)$_{6:3:1}$ anchoring. Contact times ranged from 30 s to 20 h, after which slides were briefly rinsed once with TEG and five to 10 times with water.

Vesicle Fusion. Large unilamellar vesicles (LUV) of 10 mM acrylate-PC in 20 mM sodium phosphate buffer (pH 7.4) were prepared by three successive freeze/thaw/vortex cycles using liquid N_2 and a 40 °C water bath. The LUVs were then extruded 21 times each through 2.0 μm and 600 nm polycarbonate filters and the solution diluted to 1.2 mM with 20 mM sodium phosphate buffer (pH 7.4) and 150 mM NaCl. Alkylated substrates were incubated with the vesicle solution at 37 °C for fusion times, as specified.

In Situ Photopolymerization of the Supported Lipid Film. Details of the photopolymerization of lipid films on alkylated glass have been reported elsewhere.[11] Briefly, a stock solution of co-initiators was prepared as 10 mM Eosin Y (EY), 225 mM triethanolamine (TEA), and 37 mM VP in water. A 10:1 (mol/mol) monomer/EY ratio was used for photopolymerization. Thus, 10 μL of initiator was added with stirring to the vial containing 1 mL of vesicle solution and test substrate. The vial was purged with N_2 for 15 min and the test sample irradiated with visible light at a distance of 6.5 cm for 30 min (50 mW/cm^2).

Film Stability Studies. Samples were incubated in PBS at 23 °C for periods of up to three weeks, after which they were removed and analyzed by contact angle goniometry, IR spectroscopy, or fluorescence microscopy. In addition, surfaces were examined before and after a 2-hour exposure to PBS in a parallel plate flow chamber at a wall shear rate of 2000 sec^{-1}, which is at least two orders of magnitude greater than those surface forces anticipated in a relevant in vivo setting.

Generation of Alginate Beads Coated with a Polymerized Lipid Film. *General Methods*. Microbeads ($d \sim 300$ μm) were prepared using an electrostatic bead generator (Pronova Biomedical, Inc.) set at 4.7 kV. Briefly, the alginate solution (2.0% w/v, pH 7.4), with or without cells or FITC-labeled dextran was extruded at a flow rate of 0.2 mL/min through a flat end needle with an internal diameter of 0.10 mm into a 1.1% w/v $CaCl_2$ solution.

Formation of a Membrane-Mimetic Coating. At room temperature, alginate beads were incubated with PLL (0.10% w/v) for 30 s and then rinsed twice with PBS. Beads were then incubated in dilute alginate (0.15% w/v) for 30 s followed by two brief saline rinses. This process completed a cycle of forming a single PLL-alginate bilayer and was repeated four times followed by a final 30-second incubation in PLL. The beads were then incubated in a solution containing poly(HEA_6:DOD_3:SSS_1) (0.10 mmol of SSS in 1% DMSO) for 30 s and subsequently rinsed three times with PBS.

Scheme 1. Synthesis of Polyelectrolyte Amphiphilic Terpolymer with Sulfonate Anchoring Groups.

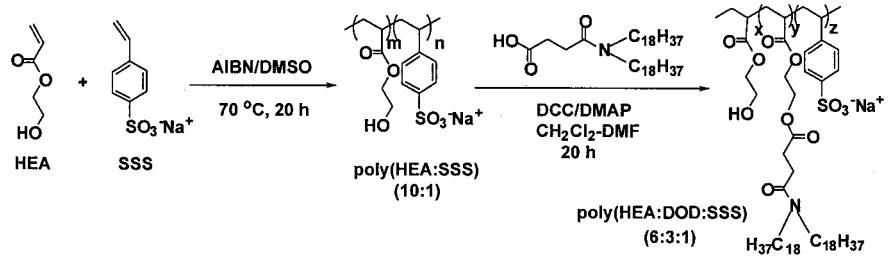

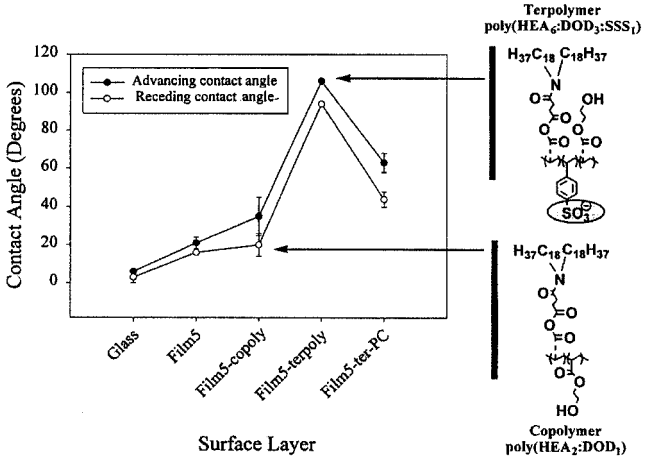

Figure 2. Advancing contact angles with successive assembly of terpolymer and lipid films on an alginate/PLL multilayer: $(alginate/PLL)_5$ = Film5; $(alginate/PLL)_5$/terpolymer = Film5-terpoly; $(alginate/PLL)_5$/terpolymer/PC = Film5-terpoly-PC. "Copoly" designates a HEA:DOD (2:1) copolymer without sulfonate anchors and demonstrates inability of the polymer to adsorb to PLL.

The formation of a supported lipid film was achieved by incubating beads (0.5 mL) in a lipid vesicle solution (1 mL) for 4 h at 37 °C with gentle mixing. At the end of the incubation period, 10 μL of a photoinitiator mixture (10 mM EY, 225 mM TEA, and 37 mM VP in water) was added. The solution was irradiated with visible light (50 mW/cm^2) for 30 min at room temperature. Beads were then rinsed three times in PBS.

Characterization of Molecular Transport across Microbeads Coated with Polymeric Membrane-Mimetic Barrier. FITC-labeled dextran of various molecular weights (9, 21, 38, 72 kD) were used to study the transport properties of the beads at various stages of polyelectrolyte and lipid membrane coating. Dextran containing beads were incubated at room temperature in saline and aliquots of the bathing solution were analyzed by UV−Vis absorption spectroscopy at timed intervals.

Viability of CHO K-1 Cells within Alginate Microbeads Coated with a Membrane-Mimetic Encapsulation Barrier. CHO K-1 cells (ATCC, Inc.) were suspended in alginate solution at a cell density of $4-6 \times 10^6$ cells/mL and extruded into a calcium chloride bath, as detailed above. The methodology of microbead formation was otherwise similar to that previously described with several modifications to maximize cell viability. Specifically, coating solutions were supplemented with glucose (3.15 g/L), unilamellar vesicles were prepared in Ham's F-12 medium without serum and phenol red, and all procedures performed, where possible, in an incubator at 37 °C and 5% CO_2. Cell viability was characterized after bead coating and after in vitro incubation periods of up to 48 h using the LIVE/DEAD Cell Viability/Cytotoxicity Kit (L-3224; Molecular Probes, Inc).

Results and Discussion

1. Synthesis of an Electrostatically Anchored Amphiphilic Polymer for Surface Alkylation. We initially investigated the copolymerization of HEA, DOD, and styrene sulfonate using a free radical polymerization scheme. To increase the solubility of styrene sulfonate in nonpolar solvents, a tetra-*n*-butylammonium (*n*-Bu_4N^+) group was used to replace sodium cation. The modified styrene monomer, SS-*n*-Bu_4N, demonstrated excellent solubility in THF, toluene, as well as chloroform. Copolymerization was performed in both THF and toluene using AIBN as a radical initiator at various monomer/initiator (M/I) molar ratios. At an M/I ratio of 20/1, 100% conversion was achieved and *n*-Bu_4N^+ in the crude reaction product was replaced with Na^+ by ion-exchange using Macroporous MSC-1 resin. However, the composition of styrene sulfonate in the afforded polymer was significantly lower than expected based on the monomer molar feed ratio. For example, with a molar feed ratio of HEA:DOD:SS-*n*-Bu_4N of 6:3:1, the molar content of styrene sulfonate varied between 0.2 and 0.9, with a characteristic value of $\sim$ 0.5. The content of styrene sulfonate improved little with an increase in the feed ratio of HEA:DOD:SS-*n*-Bu_4N, even up to 6:3:6. Nor were these results improved with successive addition of monomer or monomer pairs to the reaction vessel. Poor adsorption of the terpolymer to charged surfaces was observed when the relative molar concentration of styrene sulfonate was less than 0.9.

As a consequence of this limitation, a second approach for generating the desired terpolymer was investigated (Scheme 1). HEA and styrene sulfonate were initially copolymerized in DMSO by radical polymerization with typical yields of over 80% and with a monomer conversion of 100% at a M/I ratio of 100:1. Moreover, the molar ratio of HEA and styrene sulfonate in the resulting copolymer was in excellent agreement to the feed ratio. This copolymer was used as a precursor to the final amphiphilic polymer. Carbodiimide chemistry was used to attach the diacyl group to the copolymer via an ester linkage. Typical yields were over 70% with excellent reproducibility and agreement of product composition-to-reagent ratio.

2. Layer-by-layer Assembly of a Membrane-Mimetic Film on a Charged Hydrated Substrate. Thin films based upon the assembly of a polyelectrolyte multilayer (PEM) involve the sequential adsorption of oppositely charged polymers from dilute solution onto a substrate.[21] In the process, an interpenetrated multilayer structure is produced where film thickness is dependent upon the charge density and molecular weight of the polyelectrolyte, as well as the total number of deposited layers.[22−25] In this report, we chose to use the alginate-

(21) Decher, G. *Science* **1997**, *277*, 1232−1237.
(22) Lvov, Y.; Decher, G.; Mohwald, H. *Langmuir* **1993**, *9*, 481−486.
(23) Lvov, Y.; Haas, H.; Dechner, G.; Mohwald, H.; Kalachev, A. *J. Phys. Chem.* **1993**, *97*, 12835.
(24) Tronin, A.; Lvov, Y.; Nicolini, C. *Colloid Polym. Sci.* **1994**, *272*, 1317.

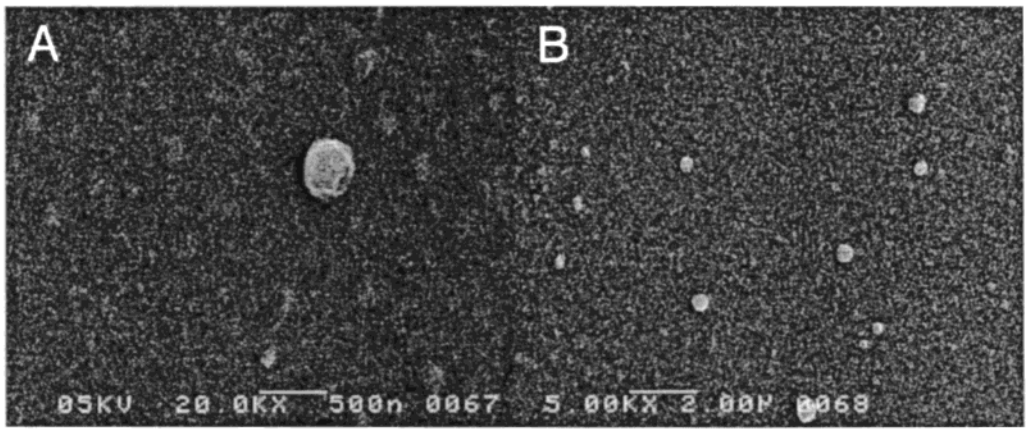

Figure 3. High-resolution in lens FESEM of a membrane-mimetic film at (A) 20,000X (scale bar = 500 nm) and (B) 5,000X (scale bar = 2 μm) magnification. An occasional vesicle is noted on the film surface.

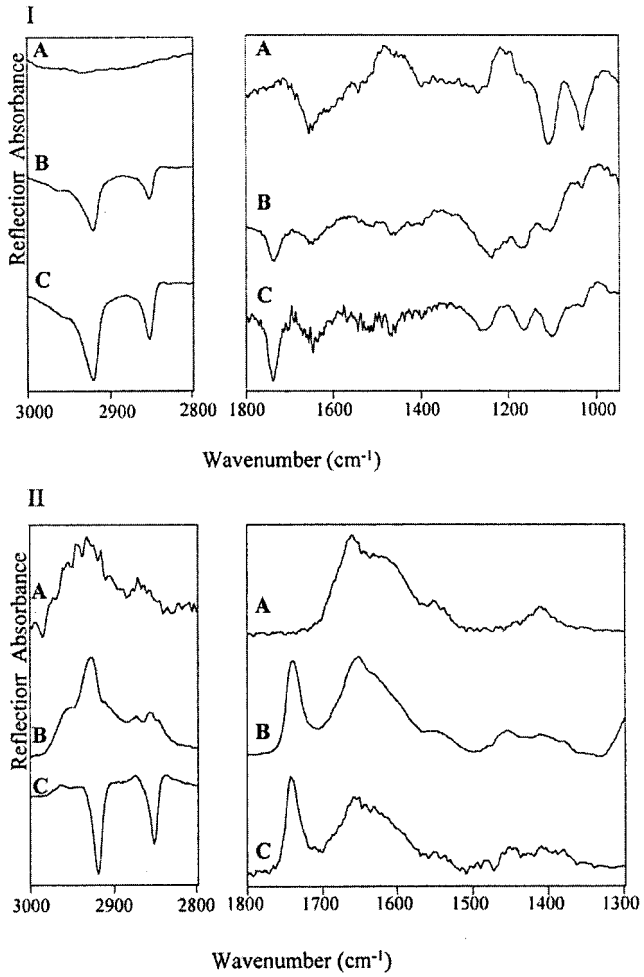

Figure 4. I. Perpendicular (R_s) polarized external reflection infrared spectra following successive adsorption of A: (PLL/alginate)$_5$–PLL; B: poly(HEA$_6$:DOD$_3$:SSS$_1$); and C: polymerized lipid film. **II.** Parallel (R_p) polarized external reflection spectra following successive adsorption of A: (PLL/alginate)$_5$–PLL; B: poly(HEA$_6$:DOD$_3$:SSS$_1$); and C: polymerized lipid film.

PLL system to generate a PEM. Alginate and PLL are negatively and positively charged polyelectrolytes, respectively, and have been the subject of intense study as complex gels, colloidal particles, and multilayers. Poly-l-lysine was always deposited last to produce a positively charged substrate for electrostatic anchoring of the negatively charged amphiphile and subsequent lipid film formation.

Table 1. Thin Film Thickness as Determined by Ellipsometry

film	thickness (Å)
Si-(PLL-Alg)$_5$-PLL	154 ± 7.5
PLL-Alg bilayer	28 ± 7.5
Si-(PLL-Alg)$_5$-PLL-Ter	206 ± 7.1
Terpolymer layer	52 ± 7.1
Si-(PLL-Alg)$_5$-PLL-Ter-PC	229 ± 4.5
PC layer	23 ± 4.5

Contact angles were measured at various stages of the film forming process (Figure 2). As anticipated, advancing contact angles were low for successive alginate (∼5°) and PLL (∼ 10° − 20°) multilayers. After the formation of three PLL/alginate bilayers, contact angles approached constant values for both layers with little change over at least 20 successive bilayers (data not shown). We also observed relatively small differences in advancing and receding contact angles over a range of PLL molecular weights (21−479 kD). In all subsequent studies, membrane-mimetic film formation was performed on a multilayer consisting of PLL (479 kD) adsorbed onto five bilayers of PLL/alginate ((PLL/alginate)$_5$–PLL).

The amphiphilic polymer, poly(HEA:DOD:SSS) was coated onto the surface of a (PLL-alginate)$_5$–PLL film with advancing contact angles exceeding 100° after incubation periods as short as 30 s. Notably, a 24-hour incubation of the substrate with a copolymer of HEA and DOD, at a similar molar concentration of DOD, did not result in significant copolymer adsorption, as confirmed by an increase in advancing contact angles from 20 to 30°. Thus, the presence of anionic sulfonate groups are critical for polymer adsorption.

The deposition of a lipid film by trough techniques is difficult to adapt to nonplanar geometries. For this reason, we chose vesicle fusion for deposition of a lipid assembly on the alkylated polyelectrolyte multilayer. After in situ photopolymerization of the deposited phospholipid layer, an advancing contact angle of ∼60° was observed, in good agreement with previous studies. These values are also consistent with prior reports of Hayward et al.[26] and Köhler et al.[27] of PC derivatized glass, as well as our own data in other polymerized lipid systems. Of note, little change

(25) Mao, G.; Tsao, Y.-H.; Tirrell, M.; Davis, T.; Hessel, V.; Ringsdorf, H. *Langmuir* **1995**, *11*, 942−952.

(26) Hayward, J. A.; Durrani, A. A.; Lu, Y.; Clayton, C. R.; Chapman, D. *Biomaterials* **1986**, *7*, 252−258.

(27) Kohler, A. S.; Parks, P. J.; Mooradian, D. L.; Rao, G. H. R.; Furcht, L. T. *J. Biomed. Mater. Res.* **1996**, *32*, 237−242.

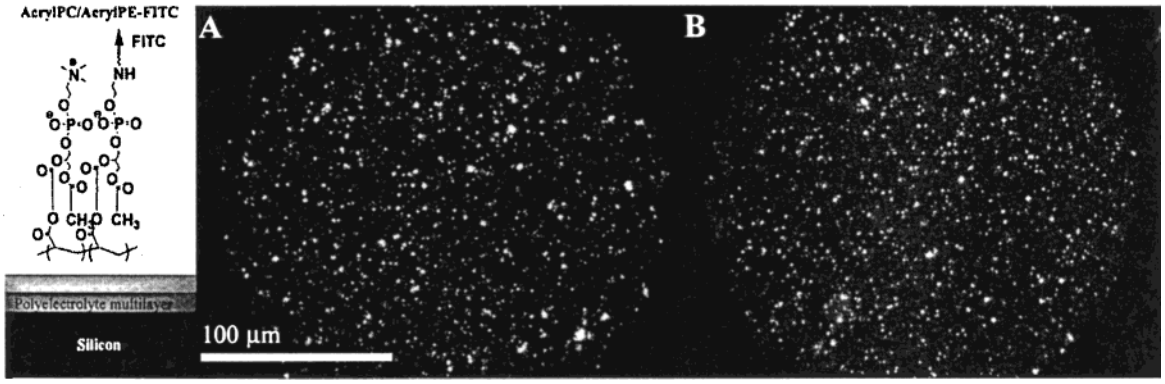

Figure 5. Fluorescent image of an alginate/PLL/terpolymer coated silicon slide after vesicle fusion and polymerization of a lipid assembly comprised of Acryl-PC and AcrylPE-FITC (1 mol %) (A). Little change is observed after a 2 h exposure to PBS at a shear rate of 2000 sec^{-1} (B).

Table 2. Angle−Dependent XPS Analysis of Multilayer Assembly during the Formation of a Supported Membrane−Mimetic Thin Film

		atomic percentage			
film	atom	15°	45°	90°	predicted[a]
	C	65.6 ± 1.7	60.8 ± 0.8	59.5 ± 2.9	62.0
$(PLL-Alg)_5$-PLL	N	9.2 ± 1.4	10.4 ± 16	9.9 ± 0.3	24.2
	O	24.2 ± 1.6	27.6 ± 1.1	28.0 ± 1.8	13.8
	C	77.7 ± 9.5	78.3 ± 1.5	75.9 ± 3.8	76.2
$(PLL-Alg)_5$-PLL-Ter	N	2.6 ± 1.4	3.8 ± 1.3	3.2 ± 1.4	1.6
	O	15.3 ± 6.4	16.2 ± 0.9	18.0 ± 1.8	21.1
	S	0.27 ± 0.05	0.8 ± 0.3	1.0 ± 0.6	1.1
	C	75.6 ± 12.7	74.2 ± 7.8	72.9 ± 5.4	76.5
	N	0.83 ± 0.7	2.1 ± 0.46	1.9 ± 1.6	2.0
$(PLL-Alg)_5$-PLL-Ter-PC	O	17.3 ± 5.8	19.0 ± 4.3	19.7 ± 3.2	19.6
	S	0	0	0	0
	P	3.7 ± 0.2	0.97 ± 0.5	0.87 ± 0.2	1.85

[a] Approximate estimate as determined by simple atom counting.

Table 3. Infrared Band Assignments for Successive Assembly of a Supported Membrane−Mimetic Thin Film

	$(PLL/alginate)_5$−PLL		$(PLL/alginate)_5$−PLL terpolymer		$(PLL/alginate)_5$−PLL TerpolymerAcrylatePC	
	(frequency cm^{-1})		(frequency cm^{-1})		(frequency cm^{-1})	
absorption mode	R_s	R_p	R_s	R_p	R_s	R_p
OH stretch	3500−3000	3500−3000	3500−3000	3500−3000	3500−3000	3500−3000
CH stretch	2934.0	2930.0				
CH_2 stretch (antisymmetric)			2925.3	2928.5	2924.3	2920.2
CH_3 stretch (symmetric)				2872.9		
CH_2 stretch (symmetric)			2854.7	2855.8	2854.1	2853.7
C═O stretch (ester)			1735.2	1739.4	1739.4	1741.5
C═O−NH stretch (amide I)	1650.3	1650.1	1647.9	1652.4	1647.3	1652.2
N−H bend of NH_3^+	∼1620−1610	∼1620−1610	∼1620−1610	∼1620−1610	∼1620−1610	∼1620−1610
COO− antisymm stretch		1550.0		1549.0 (sh)		1548.0
CH_2 bend (scissoring)			1466.7	1456.4	1467.4	1461.1
COO− symm stretch		1409.2		1408.0		1402.8
PO_{2-} symm + CO−O−C ymm stretch					1262.6	
CO−O−C antisym stretch			1172.2		1164.6	
CO−O−C symm stretch			1104.9		1101.1	
C−O stretch	1110.7, 1031.5		1030.0 (weak)		1026.3 (weak)	

in contact angles were observed during a three week incubation period in PBS.

Additional surface sensitive techniques afforded further insight into film properties. High resolution in-lens FESEM provided a convenient method to examine surface topography over large film areas (Figure 3). While occaisional vesicles were noted on the film surface, little overall surface roughness was observed. Ellipsometry was used to measure the hydrated thickness of each film layer (Table 1) and XPS to further define atomic level surface properties (Table 2). A thickness of 28 Å was observed per alginate-PLL bilayer and is consistent with prior reports of this system. The thickness of the adsorbed terpolymer was 52 Å and the thickness of the supported lipid film was 23 Å. This value compares favorably with measurements determined by X-ray diffraction[28] or neutron reflectivity[5] for liquid-crystalline DPPC multilayers and supported monolayers, respectively. XPS confirmed that after the deposition of five or more alginate-PLL bilayers, surface Si was no longer observed. Significantly, sulfur was identified after terpolymer adsorption and phosphorus demonstrated after lipid vesicle fusion and polymerization (Table 2).

3. Structural Characterization of the Supported Lipid Assembly by Infrared Spectroscopy. Infrared

(28) Nagle, J. F.; Zhang R.; Tristram-Nagle, S.; Sun, W.; Petrache, H. I.; Suter, R. M. *Biophys. J.* **1996**, *70*, 1419−1431.

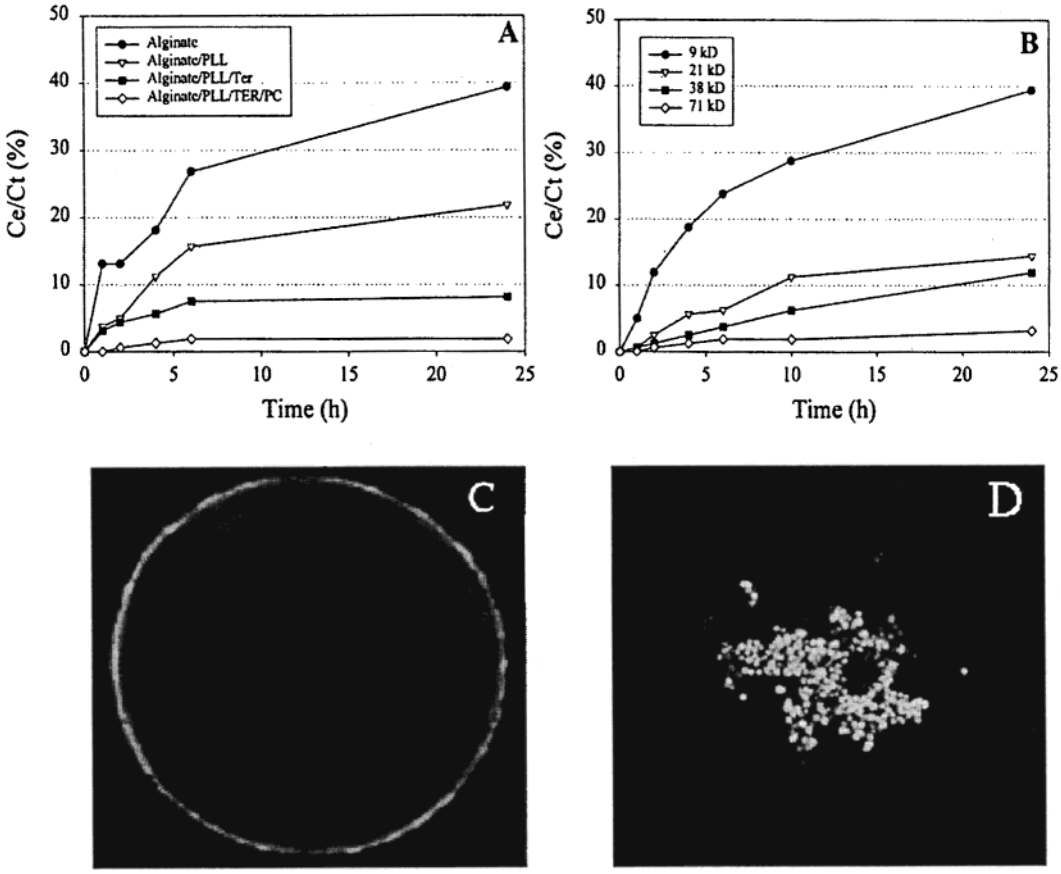

Figure 6. (A) Release rate of encapsulated 71 kD FITC-dextran from alginate beads following successive adsorption of (PLL/alginate)$_5$–PLL; poly(HEA$_6$:AOD$_3$:SSS$_1$), and a polymerized lipid film. (B) Release rates of encapsulated FITC-dextrans (MW 9, 21, 38 kD) from alginate-PLL microbeads coated with a photopolymerized membrane-mimetic barrier (T 23 °C). (C) Fluorescent image of an alginate/PLL microbead (d ~ 300 μm) coated with Acryl-PC and AcrylPE-FITC (1 mol %). (D) Fluorescent image of CHO K-1 cells 24 h after encapsulation in a membrane coated alginate/PLL microbead. Cells were stained using Live/Dead cell assay (green − viable; red − nonviable).

spectra were acquired during each stage of film construction in order to identify functional group characteristics that were unique to each film component, as well as to provide insight into acyl chain orientation. Significantly, this analysis provides both a framework for characterizing film stability under varying environmental conditions and establishes the level of disorder within the supported lipid assembly. This latter feature may have an important impact on film properties, including membrane permeability and the capacity to organize and appropriately orient membrane based proteins. The perpendicular (R_s) and parallel (R_p) polarized external reflection spectra are presented in Figure 4 and Table 3.

Notably, the polarized IR spectra of the PLL-alginate multilayer revealed PLL-dependent bands including an amide I stretch and a shoulder containing the N−H stretch of $-NH_3^+$ (1650, 1615 cm^{-1}, respectively). The symmetric (1410 cm^{-1}) and antisymmetric (1550 cm^{-1}) stretching vibrations of the carboxylate ion (COO^-) are unique to alginate and could be resolved in the R_p polarized spectra. A broad and strong −OH vibration, due to alginate, was observed between 3600 and 3000 cm^{-1}.

Addition of the terpolymer (Figure 4B) was associated with intense symmetric and antisymmetric methylene stretches, located from 3000 to 2800 cm^{-1}, as well as an ester carbonyl band centered at 1734 cm^{-1}. These vibrations can be attributed to DOD and HEA groups, respectively. The spectral intensity of unique PLL (amide I stretch) and alginate (antisymmetric and symmetric COO^- stretches) vibrations were reduced, but remain identifiable.

Dramatic changes in the R_s and R_p polarized IR spectra were seen after fusion and lipid polymerization (Figure 4C). A band at ~1263 cm^{-1} is noted in the R_s polarized spectrum. This band results from the antisymmetric P=O stretch and its intensity increases because of the ν_a and ν_s CH_2, the C=O (ester carbonyl), and C=O−O−C stretching absorption modes (1120−1105 cm^{-1}). These were observed in both polarized spectra. The latter absorption modes were present in both lipid and terpolymer components.

The most notable difference, however, occurs in the ν_a and ν_s CH_2 stretching modes of the R_p polarized spectrum where the bands go from positive to negative intensity after lipid deposition and polymerization (Figure 4II, B and C). Positive and negative absorption bands have been theoretically predicted and experimentally observed in studies of monomolecular thin films coated onto silicon and other semiconductor substrates.[29−32] Moreover, we have observed this behavior in a recent investigation of a polymeric lipid film deposited on OTS/Si.[21] Using theoretical reflection−absorption plots generated from Fresnel reflection equations for a three-phase system,[33,34] we correlated, qualitatively and quantitatively, positive and negative absorption modes with the molecular orientation

(29) Dluhy, R. A. *J. Phys. Chem.* **1986**, *90*, 1373−1379.
(30) Wong, J. S.; Yen, Y.-S. *Appl. Spectrosc.* **1988**, *42*, 598−604.
(31) Mielczarski, J. A.; Yoon, R. H. *J. Phys. Chem.* **1989**, *93*, 2034−2038.
(32) Yen, Y.-S.; Wong, J. *J. Phys. Chem.* **1989**, *93*, 7208−7216.
(33) Hasegawa, T.; Takeda, S.; Kawaguchi, A.; Umemura J. *Langmuir* **1995**, *11*, 1236−1243.
(34) Sakai, H.; Umemura, J. *Langmuir* **1998**, *14*, 6249−6255

of the alkyl chains of OTS and the supported lipid.[11] A similar approach provided insight into the structure of membrane-mimetic film described in this current report.

The positive methylene absorption bands in the Rp polarized external reflection spectra (Figure 4B) indicate that the molecular orientation of the terpolymer alkyl chains is random and tilted away from the surface normal. This is also supported by the frequency position of the methylene stretching vibrations, which are indicative of hydrocarbon chain order.[35−37] Specifically, the average positions of the methylene symmetric (ν_s CH_2) and antisymmetric (ν_a CH_2) stretching modes in the R_s polarized spectra are 2854.7 and 2925.3 cm^{-1} (Figure 4B). These positions imply that the hydrocarbon chains are likely disordered and possess both trans and gauche conformers. This is not altogether unexpected as the alkyl chains present in the terpolymer are relatively long and may not be tightly packed together because of the HEA spacer groups (Figure 1).

After fusion and polmerization of the acrylate-PC assembly, the methylene absorption bands reversed in intensity. Qualitatively, this result indicates that the acyl chain tilt is closer to the surface normal. Presumably, the mobile hydrocarbon chains of the terpolymer are now held to a smaller chain tilt because of van der Waal interactions with associated lipid acyl chains. Using a film thickness determined by ellipsometry and a previously described calculation procedure,[11] we determined that the average orientation after the addition of the lipid is 39.5°. This result undoubtedly includes the orientation of both lipid and terpolymer alkyl chains. The increase in chain order and orientation is also supported by the frequency position of the methylene symmetric and antisymmetric stretching vibrations, which were 2853.9 and 2922.3 cm^{-1}, respectively. The addition of the acrylate-PC film is associated with a conformational ordering of the hydrocarbon chains, which coincides with an increase in the hydrocarbon chain tilt. Of note, chain tilts of 34° and 38° have been observed for nonpolymerized lipid monolayers of DPPC when produced on a self-assembled monolayer of octadecanethiol on gold by Langmuir-Schäefer or vesicle fusion methods, respectively.[5] Thus, a significant degree of acyl chain order can be maintained even after polymerization of the lipid assembly.

4. A Polymeric Lipid Film, Assembled on a Polyelectrolyte Multilayer, is Stable in a High Shear Flow Environment. At each stage of the coating procedure, films were exposed to PBS at a wall shear rate of 2000 sec^{-1} for a 2-h contact period. Polarized IR spectra were unchanged with the exception of the terpolymer-coated sample in which significant chain ordering was induced by exposure to high shear (data not shown). To further enhance our ability to visually monitor film stability, we designed an acrylate functionalized phosphatidylethanolamine, which allowed the introduction of FITC by acylation of the amine group. Thus, vesicles doped with 1 mol % of mono-AcrylPE-FITC were fused onto the terpolymer-coated substrates and exposed to flow (Figure 5). No discernible loss of fluorescent signal was observed.

5. Barrier Permeability is Modulated by Coating with a Membrane-Mimetic Film. The release of encapsulated 71 kD FITC-dextran as related to layer-by-layer deposition of film components is presented in Figure 6A. A progressive decrease in the rate and magnitude of dextran release was observed with the addition of each successive film layer. While little release of 71 kD dextran was noted following the formation and polymerization of the supported lipid film, the release of lower molecular weight dextrans (9, 21, and 38 kD) was observed (Figure 6B). Nonetheless, the addition of a membrane-mimetic coating provides an opportunity to control not only the chemical and biological functionality of the surface, but interfacial transport characteristics, as well. For example, while an accepted standard for an ideal molecular weight cutoff does not currently exist for the design of an immunoisolation barrier, our studies demonstrate that an ultrathin polymeric membrane-mimetic coating can yield a stable interface which is likely impermeable to immunoglobulins (MW 150 kD), while allowing the release of secreted bioactive proteins, such as insulin (11 kD) that would be required in the case of encapsulated pancreatic islets.

6. Encapsulated Cell Viability is Maintained during the Assembly and Polymerization of a Membrane-Mimetic Coating. The impact of materials, procedures, and conditions required for membrane-mimetic film formation on cell viability was analyzed using alginate encapsulated CHO cells. In preliminary studies, approximately 50% of cells survived encapsulation when alginate, PLL, amphiphilic polymer, and lipid vesicles were prepared in PBS alone. To improve cell survival, glucose was added to all PBS, alginate, and PLL solutions and both polymer adsorption and vesicle fusion steps were performed in Ham's F-12 medium without serum and phenol red. In addition, with the exception of vesicle fusion, all coating and rinse procedures were performed using ice-chilled solutions, so as to lower the metabolic demands of the cells. This strategy had no effect on membrane structure or properties. The ability to produce a stable, uniform membrane-mimetic film on bead surfaces was demonstrated through doping of the membrane-mimetic film with a FITC-labeled lipid (Figure 6C). The result was that transport properties were unchanged, and overall cell viability exceeded 90% (Figure 6D).

Conclusions

A stabilized, polymeric membrane-mimetic surface was produced on an alkykated polyelectrolyte multiplayer by in-situ photopolymerization of a lipid assembly. Molecular characterization confirmed the generation of a well-ordered, supported lipid monolyer, which was stable under high shear flow conditions and capable of modulating interfacial molecular transport. In addition, the ability to use this system as a cell encapsulation barrier is illustrated. In principle, the addition of a stable, supported lipid membrane provides an additional mechanism for controlling both physiochemical and biological properties of a polyelectrolyte multilayer. In the process, a strategy is established for further optimizing the clinical performance characteristics of artificial organs and other implanted medical devices.

Acknowledgment. This work was supported by grants from the NIH, and the Debbie Roos Hoppenfeld Memorial Research Award from the JDRF. The authors wish to acknowledge the Emory University Mass Spectrometry Center, which was funded by grants from the NIH and NSF. We also thank Professor Joseph A. Gardella, Jr. and Dr. Richard Nowak at SUNY Buffalo for XPS measurements.

LA011254G

(35) Tasumi, M. S.; Miyaza, T. J. *J. Mol. Spectrosc.* **1962**, *9*, 621.
(36) Snyder, R. G.; Hsu, S. L.; Krimm, S. *Spectrochim. Acta, Part A* **1978**, 34A, 395−406.
(37) Painter, P. C., Coleman, M. M., Koenig, J. L. *The Theory of Vibrational Spectroscopy and its Application to Polymeric Materials*. John Wiley & Sons: New York, 1982.